Maxwell-Wagner-Sillars effects on the thermal-transport properties of polymer-dispersed liquid crystals

M. Kuriakose, S. Longuemart, M. Depriester, S. Delenclos, and A. Hadj Sahraoui*

Univ. Lille Nord de France, F-59000, France; ULCO, UDSMM, F-59140 Dunkerque, France; and Unité de Dynamique et Structure des Matériaux Moléculaires, EA 4476, F-59140 Dunkerque, France

(Received 2 August 2013; revised manuscript received 13 December 2013; published 24 February 2014)

We present the depolarization field effects (Maxwell-Wagner-Sillars effect) for the thermal transport properties of polymer dispersed liquid crystal composites under a frequency-dependent electric field. The experiments were conducted on polystyrene/4-Cyano-4′-pentylbiphenyl (PS/5CB) PDLCs of 73 vol.% and 85 vol.% liquid crystal (LC) concentrations. A self-consistent field approximation model is used to deduce the electrical properties of polymer and LC materials as well as the threshold electric field. Electric field-varying (at constant frequency) experiments were also conducted to calculate the interfacial thermal resistance between the LC droplets and polymer matrix as well as to find the elastic constant of LCs in droplet form.

DOI: 10.1103/PhysRevE.89.022511 PACS number(s): 42.70.Df, 44.10.+i, 44.35.+c, 66.30.hk

I. INTRODUCTION

Polymer dispersed liquid crystals (PDLCs) are made of micron or submicron liquid crystal (LC) droplets encapsulated in a polymer matrix. Their much better performance than conventional LC displays as well as their broad application potential such as in flexible displays [1–3], window shutters, projection displays [4], optical switches [5], focus-tunable lenses [6], etc., have led the scientific world to consider this as a promising candidate in technology. The usual operation of PDLCs is dependent on changing the film transparency to the visible light from an opaque (OFF) state to a transparent (ON) state by the application of an external electric field (EF). The reason for such behavior is the mismatch in refractive indexes between LC droplets and the polymer matrix, which scatters away the incident light in an OFF state. Upon the application of an external EF, LC droplets modify their molecular alignment so that the refractive indexes of the host polymer layer and the LC droplets match each other in the direction of the EF. This makes the film transparent in that direction. A vast amount of studies on PDLCs' electro-optic properties have been done by various research groups to quantify and improve PDLC performance. Nevertheless their inherent structural complexities and, at the same time, the possibility to control their physical properties via external means (e.g., by applying an electric field) have led researchers to consider them as a research interest.

In composite materials, PDLCs are different from other types of composites (e.g., metallic particles in polymers) because they give the opportunity to change their transport properties via applying an EF without changing the amount, shape, or size of inclusions (LC) in a material sample under investigation. This behavior is particularly useful while studying thermal transport through composites.

Our previous studies [7] of PS/5CB PDLC samples show that the heat transport through PDLCs are affected both by the presence of an external EF and because of the variation in LC volume fraction. Here the sample's thermal conductivity increased monotonically and reached a saturation value with respect to an increase in the applied EF. This change in thermal conductivity is due to the reorientation of LC droplet directors from their random orientations to the direction of the applied field, which is in parallel to the direction of heat flow through the material sample. In order to prevent the effects of depolarization fields, an EF of 1 kHz sinusoidal wave was used in such experiments.

In this paper we report on the effects of depolarization fields (Maxwell-Wagner-Sillars effect) on thermal transport through PDLC samples. We selected PS/5CB composites for our studies because of their well-known thermo-physical properties. Recently the photothermal radiometry technique (PTR) has been demonstrated as a simple and capable technique for measuring dynamic thermal parameters of liquid samples with high precision and resolution [8]. In particular, the noncontact capability of the PTR technique helps to extract the thermal parameters from EF-varying experiments with fewer precautions, whereas many efforts are required with contact techniques, such as photopyroelectric (PPE), to facilitate experiments free from EF-induced errors.

II. MAXWELL-WAGNER-SILLARS EFFECT

Depolarization field effects in heterogeneous systems were first highlighted by Maxwell and later modified successively by Wagner and Sillars. So the interfacial polarization effects are often termed the Maxwell-Wagner-Sillars (MWS) effect [9,10]. In a heterogeneous mixture of LC droplets and a polymer matrix, due to the differences in their dielectric characteristics (ability to hold charges) as well as electrical conductivities, an additional charge accumulation occurs at each LC-polymer boundaries when the material is under an external EF, as shown in Fig. 1.

At low enough frequencies of the applied alternating field, the charges, near each LC-polymer boundary, start to build up (conductivity effect) and oppose the external EF. As a consequence, the effective field acting on the LC droplets reduces its strength. This in turn conversely affects the reorientation of the droplets and causes a decrease of the heat flow through it, in other words through the PDLC film, in the direction of the EF. The depolarization field effects in such multiphase systems vanish at sufficiently high frequencies of

*hadj@univ-littoral.fr

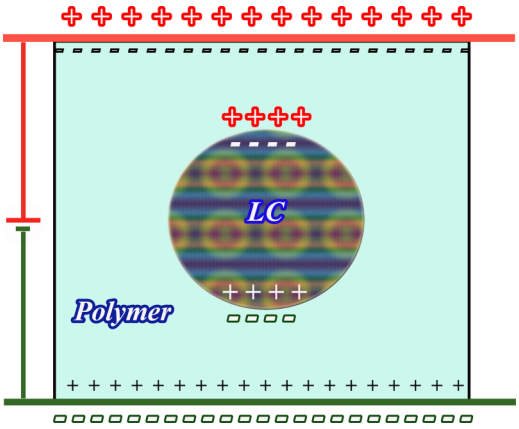

FIG. 1. (Color online) Maxwell-Wagner-Sillars effect in an heterogeneous medium. The simplest case with a single LC droplet surrounded by a host polymer matrix.

an applied EF because the movement of charges will be frozen out at high frequencies and the development of depolarization fields gets interrupted.

Several electro-optic experimental studies are reported on the interfacial polarization effects in PDLCs [11–13]. Bousoualem *et al.* [14,15] conducted studies on polystyrene/4,4′-octylcyanobiphenyl (PS/8CB) and PS/5CB dispersed systems and reported on their frequency-dependent behavior attributed to the MWS effect. Their studies, on the light transmission vs frequency of the applied EF, were modeled using a self-consistent field approximations for calculating the average electric field (E_{drop}) acting on spherical LC droplets in a PDLC sample. The equation, taking into account the MWS effect and relating the average droplet electric field, E_{drop}, to the applied EF, E_a, is given by [16,17]

$$E_{\text{drop}}(\omega_e) = \frac{3\epsilon_M^\star}{\epsilon_{\text{LC}}^\star + 2\epsilon_M^\star - \phi_{\text{LC}}(\epsilon_{\text{LC}}^\star - \epsilon_M^\star)} E_a \tag{1}$$

and

$$\epsilon_M^\star = \epsilon_M' - i\frac{\sigma_M}{\omega_e \epsilon_0}, \tag{2}$$

$$\epsilon_{\text{LC}}^\star = \epsilon_{\text{LC}\|}' - i\frac{\sigma_{\text{LC}\|}}{\omega_e \epsilon_0}, \tag{3}$$

where $\omega_e = 2\pi f_e$ and f_e is the frequency of the applied EF; ϕ_{LC} is the phase-separated LC fraction; E_a is the magnitude of the applied electric field; ϵ_M' and σ_M are the dielectric permittivity and electrical conductivity of the polymer matrix, respectively; and $\epsilon_{\text{LC}\|}'$ and $\sigma_{\text{LC}\|}$ are dielectric permittivity and electrical conductivity of the LC in the direction of E_a, respectively.

Inside PDLC, a part of the LC dissolves into the polymer. A maximum amount of the LC dissolved in a polymer matrix is defined as the solubility limit (β), and it can be found by performing differential scanning calorimetry measurements. The undissolved portion of the LC forms droplets. Knowing β and the amount of LC added to the polymer (x), we can calculate the phase-separated LC fraction (ϕ_{LC}) using [18–20]

$$\phi_{\text{LC}} = \frac{100}{x}\frac{x-\beta}{100-\beta}, \quad x \geqslant \beta, \tag{4}$$

where all the quantities are in a volume percentage. The value of $\beta = 55\%$ was used to calculate ϕ_{LC} in our experiments [14].

III. SAMPLE PREPARATION

Polymer dispersed liquid crystal (PDLC) samples were prepared using polystyrene (Sigma-Aldrich, molecular weight of 44 000 g/mol) as the polymer matrix and 5CB (Merck) as the inclusion with two different volume fractions, LC:PS (85:15 and 73:27). Some of the advantages of PS compared to other thermoplastic compounds are a very low ac electrical conductivity ($\sigma_{\text{ac}} \approx 10^{-9}$ S/m at 1 kHz) and uniform dielectric permittivity ($\epsilon_M' \sim 2.5$) in both temperature (25–80 °C) and frequency [21,22]. The density (ρ) of PS and 5CB are ≈ 1 ($\rho_{\text{PS}} = 1.047$ kg/m^3 and $\rho_{\text{5CB}} = 1.008$ kg/m^3). Dielectric permittivity and ac electrical conductivity of 5CB are $\epsilon_{\text{LC}\|}' = 10$ and $\sigma_{\text{LC}\|} = 10^{-8}$ S/m [23,24]. The temperature range of the nematic phase of 5CB is between 23 and 35 °C [25]. Thermal conductivity values for the PS matrix, $\kappa_m = 0.11$ W/mK, as well as for 5CB, aligned in parallel (long axis of LC molecules aligned in parallel to the heat flow direction), $\kappa_{\text{LC}\|} = 0.24$ W/mK, and perpendicular (long axis of LC molecules aligned perpendicular to the heat flow direction), $\kappa_{\text{LC}\perp} = 0.12$ W/mK, are taken from Refs. [26,27].

PDLC samples were prepared by a solvent-induced phase separation [28] procedure. At first, the required amount of both materials (5CB and PS) completely dissolved with an equal amount of chloroform. The mixture was placed in an oven for more than 24 h for a complete evaporation of solvent to obtain the final PDLC sample. Upon solvent evaporation, LC-PS phase separation happens, and 5CB droplets on the order of micron or submicron sizes develop throughout the entire polymer matrix. Micrographs of as prepared PDLCs for both LC:PS concentrations are shown in Fig. 2. The pictures were taken using a polarizing microscope with crossed polarizers.

IV. EXPERIMENTAL

We have used an improved photothermal radiometry (PTR) technique [8,29] for measuring thermal parameters of PDLC samples. The experiments were done using the back-PTR (B-PTR) configuration because of its high sensitivity and simultaneous detectability to both the thermal diffusivity and effusivity of the sample under investigation. The experimental arrangement for the sample-cell assembly is shown in Fig. 3. The sample was kept between a CaF_2 window on the top and a quartz precision cell (backing) on the bottom. An internally modulated laser ($\lambda = 532$ nm, He-Ne, Ventus HP 532, 1.4 mm spot size) source was used to generate heat at the backing-sample interface with the help of a thin ($\approx$500 nm thickness), opaque, laser-absorbing coating layer. The thermal waves diffuse into the sample and reach the top layer where a second coating, at the sample-CaF_2 interface, emits the infrared signal. The generated signal from the top CaF_2-sample interface contains the thermal information of the sample-cell assembly. It has been detected by the aid of a liquid nitrogen-cooled HgCdTe infrared detector (Judson Technologies, model J15D12-M204-S01M-60, bandwidth, dc, 250 kHz). Since the CaF_2 window is transparent to both the visible and infrared wavelengths of light, it acts as a semi-infinite top layer in the

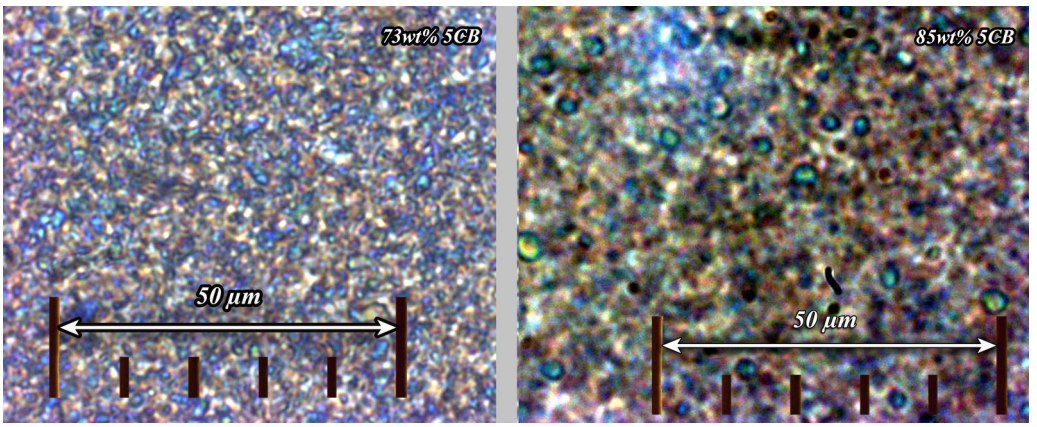

FIG. 2. (Color online) PDLC micrographs under microscope with crossed polarizers. Images of PS:5CB = 27:73 (73% LC) (left) and PS:5CB = 15:85 (85% LC) (right).

thermal configuration and passes the generated infrared signals directly to the detector.

Generally, in PTR experiments, two separate signals as a function of the laser modulation frequency (a sample scan and a reference) are used to obtain a normalized signal (by the complex division of two signals). This normalized signal, which is free from the instrumental transfer function, is analyzed to find the thermal properties of the sample under investigation while knowing the thermal properties of surrounding layers. Since B-PTR technique has the ability to find thermal parameters from a single laser modulation frequency, we have done experiments by fixing the laser modulation frequency and scanning the sample under varying EF or frequency-dependent EF (f_e). Thus, a sample's thermal diffusivity, as a function of EF or f_e, can be calculated from the phase data and the effusivity from the combined amplitude and phase signals, provided that the sample is at a quasithermally thick ($\mu_s \approx d$) regime. The analytical expressions for a sample's thermal diffusivity (α_s) and thermal effusivity (e_s) are given by [8]

$$\alpha_s = \left(\frac{d\sqrt{\alpha_r \pi f}}{d\sqrt{\pi f} - \theta\sqrt{\alpha_r}} \right)^2, \tag{5}$$

$$e_s = -\frac{1}{2}\{L - R + \sqrt{(L-R)^2 - 4J}\}, \tag{6}$$

where

$$R = \frac{e^{\theta}}{e_r A}\left(e_r^2 + e_r L + J\right), \quad L = e_c + e_b, \quad J = e_c e_b;$$

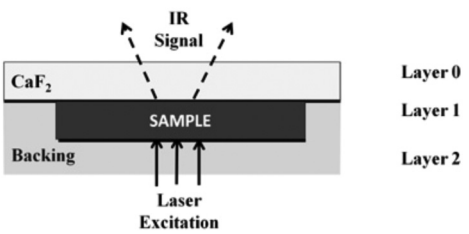

FIG. 3. Back-PTR configuration.

here A is the normalized amplitude and θ is the normalized phase, and e_r, e_s, e_c, and e_b are the thermal effusivities of the reference, sample, CaF_2 window, and backing, respectively. α_s and α_r are the thermal diffusivities of the sample and reference, respectively. f represents the modulation frequency of the laser source, and d is the sample thickness.

In order to facilitate the experiments, the required amount of the PDLC sample was cast into the quartz precision cell using a spatula, prearranged with electric contacts for the electro-thermal measurements, and heated to the matrix-softening temperature, and we closed the cell with a CaF_2 window. The measurements were carried out by keeping the

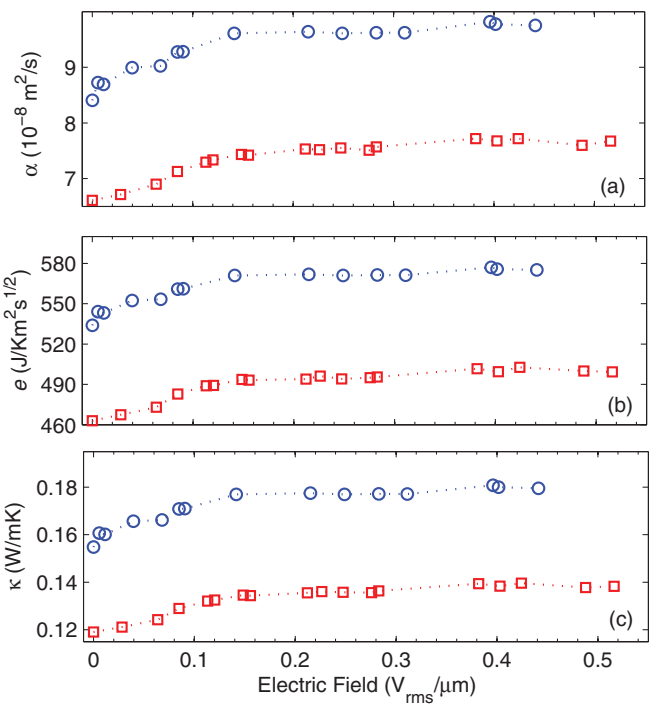

FIG. 4. (Color online) Variation of thermal diffusivity (a), thermal effusivity (b), and thermal conductivity (c) as a function of the applied electric field (at constant frequency, f_e, 1 kHz) for PDLC samples with 85% LC (blue circles) and 73% LC (red squares).

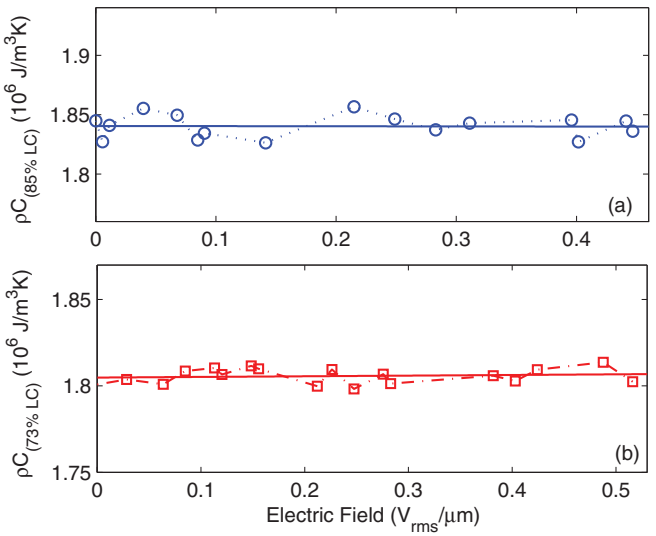

FIG. 5. (Color online) ρC plotted as a function of EF for PDLC samples with 85% LC (a) and 73% LC (b). Experimental data points for 85% LC (blue circles) and for 73% LC (red squares) along with the mean values of ρC (solid lines).

sample temperature constant at $\sim$28 °C in order to avoid temperature-dependent thermal property changes. The sample cell thickness used was $50 \pm 2\mu$m.

V. RESULTS AND DISCUSSION

The first part of the experiments on PDLCs were done with varying amplitude of the applied EF at fixed frequency ($f_e = 1$ kHz). These results are used to find the role of interfacial thermal resistance between the polymer matrix and LC droplets. The second part of the experiments deals with the frequency dependence on the thermal properties of PDLCs.

A. PDLC under a varying electric field

We have investigated the variation of thermal parameters of PDLC samples (85% LC and 73% LC) under varying electric field at constant frequency ($f_e = 1$ kHz), and the results are depicted as shown in Fig. 4. The PTR experiments were conducted by fixing the laser modulation frequency, $f = 18$ Hz, at which the sample is in a quasithermally thick regime, and varying the EF strength successively. The displayed results (Fig. 4) are from the mean of three consecutive EF scans. Additional filtering has also been done by plotting the volumetric heat capacity ($\rho C = e/\sqrt{\alpha}$) and by taking data points lying within $\pm 1\%$ or $\pm 0.55\%$ (depending on the population of experimental data points) from the linear fit value of ρC as shown in Fig. 5. Here the behavior of ρC is independent of the applied electric field as expected since the molecular reorientation in LCs does not make any contributions towards ρC, and hence it stays unchanged. Nevertheless, a change in concentration of the liquid crystals in PDLC produces a shift in the volumetric heat capacity value.

1. *Effective medium theory and interfacial thermal resistance*

In heterogeneous mixtures, the presence of interfaces and thereby an interfacial thermal resistance hinder heat transport through boundaries. Nan *et al.* [30] gave an estimation of effective thermal conductivity in heterogeneous mixtures with spherical inclusions on the basis of an effective medium approach, which has taken into account interfacial thermal resistance, and it is given by

$$\kappa_{\mathrm{PDLC}} = \kappa_m \frac{\kappa_{\mathrm{LC}}(1+\gamma) + 2\kappa_m + 2\phi_{\mathrm{LC}}[\kappa_{\mathrm{LC}}(1-\gamma) - \kappa_m]}{\kappa_{\mathrm{LC}}(1+\gamma) + 2\kappa_m - \phi_{\mathrm{LC}}[\kappa_{\mathrm{LC}}(1-\gamma) - \kappa_m]}, \tag{7}$$

where $\gamma = r_k/r_d$ is the ratio of the Kapitza radius (r_k) to droplet radius (r_d). κ_m and κ_{LC} are thermal conductivities of the polymer matrix and LC, respectively. The quantity γ is a dimensionless parameter which compares the Kapitza radius, r_k, to the droplet radius, r_d. The Kapitza radius is related to thermal interfacial resistance, and it can be considered as a quantity which indicates whether the interfaces play a significant role in the heat transport through the material composite. If $\gamma \ll 1$, the influence of the interfaces may be ignored, but if $\gamma > 1$ the contribution of the interfaces to the effective thermal conductivity becomes more important than that of the volume of the inclusions.

By knowing the thermal conductivities of the polymer matrix and LC as well as by experimentally finding κ_{PDLC} and ϕ_{LC} [Eq. (4)], one can calculate γ by rearranging Eq. (7), which is given by

$$\gamma = \frac{(\kappa_m/\kappa_{\mathrm{PDLC}})(\kappa_{\mathrm{LC}} + 2\kappa_m + 2\phi\kappa_{\mathrm{LC}} - 2\phi\kappa_m) - \kappa_{\mathrm{LC}} - 2\kappa_m + \phi\kappa_{\mathrm{LC}} - \phi\kappa_m}{2\kappa_{\mathrm{LC}} + \phi\kappa_{\mathrm{LC}} + 2(\kappa_m\kappa_{\mathrm{LC}}/\kappa_{\mathrm{PDLC}})(\phi_{\mathrm{LC}} - 1)}. \tag{8}$$

Equation (8) allows us to compute r_k, once we know the mean radius of the droplets. Micrographs obtained from a polarized microscope, for both samples (Fig. 2), are used for the estimation of droplet sizes. The majority of the droplets lie within diameters of 1–5 μm for the 85% LC sample and 0.5–2 μm for the 73% LC sample.

2. *Order parameters of PDLC film*

Considering the thermal anisotropy of the nematic LC phase, the effective thermal conductivity of the PDLC depends on the average orientation of the LC molecule with respect to the heat flow direction. For PDLC systems, two order parameters must be considered. Zumer and Doane [31] introduced the notion of droplet director $\hat{n}_D$. The order can be quantified for each droplet as the deviation of the molecule from this director. The droplet's order parameter, S_D, can be defined as

$$S_D = \left\langle \tfrac{1}{2}\{3[\hat{n}_D \cdot \hat{n}(\hat{r})]^2 - 1\} \right\rangle,$$

where $\hat{n}(\hat{r})$ denotes the local nematic director and $\langle\rangle$ is the averaging over the ensemble of molecules of the droplet.

Usually, in PDLCs zero field droplet directors are randomly distributed over all the sample. The effective thermal

conductivity will thus depend on these droplets' director distribution, and one may define as well a sample order parameter S_S:

$$S_S = \left\langle \tfrac{1}{2}[3(\hat{n}_D \cdot \hat{z})^2 - 1] \right\rangle = \left\langle \tfrac{1}{2}(3\cos^2\theta - 1) \right\rangle,$$

where $\hat{z}$ denotes the heat flow direction or the applied EF direction and θ the angle between the droplets' director and the $\hat{z}$ axis, the average being done over all the droplets of the sample.

Finally, the effective thermal conductivity of the LC phase in response to the applied electric field may be expressed as

$$\kappa_{LC} = \kappa_\perp + \tfrac{1}{3}(1 + 2\,S_S\,S_D)\Delta\kappa \qquad (9)$$

with $\Delta\kappa = \kappa_\parallel - \kappa_\perp$ the thermal anisotropy of the liquid crystal, and $\kappa_\parallel$ and $\kappa_\perp$ the thermal conductivity along or perpendicular to the molecular axis. Interestingly, Eq. (9), which we obtained for the effective thermal conductivity of LC droplets, is similar to the equation for the average dielectric constant of LC droplets in PDLC [32,33].

The behavior of the thermal conductivity (Fig. 4) is intimately linked with the reorientation of molecules in LC droplets. The application of an electric field will facilitate the orientation of the droplet directors along this direction and thus will increase the order parameter S_S leading to a higher effective thermal conductivity as $\Delta\kappa$ is positive. For sufficiently high electric fields, all droplet directors align with the external field ($S_S = 1$) and the thermal conductivity reaches a maximum value.

For PS/5CB PDLC, nematic droplets possess the bipolar configuration; at a zero field the nematic is aligned tangentially at the droplet wall [Fig. 6(a)]. Upon application of the field, the nematic within the center of each droplet aligns quickly with the field. This process leads to a droplet, where the bulk of the nematic is aligned with the applied field, but near the wall of the droplets the nematic molecules are still aligned tangentially to the droplet surface [Fig. 6(b)]. This bipolar configuration corresponds to the calculated value of $S_D = 0.7$ for spherical droplets, which remains unchanged upon application of an electric field [32]. The orientation of the molecules along the surface of the droplets remains unchanged in the presence and in the absence of the electric field; this led us to consider that the thermal interfacial resistance is constant and independent of the electric field. For calculating γ, we have used thermal

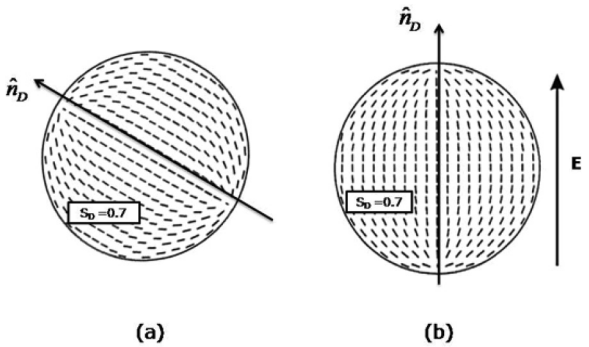

FIG. 6. Schematic of the bipolar droplet alignment in a nematic phase (a) at a zero field (droplet director can align in any direction) and (b) at a high field (director aligns parallel to the EF).

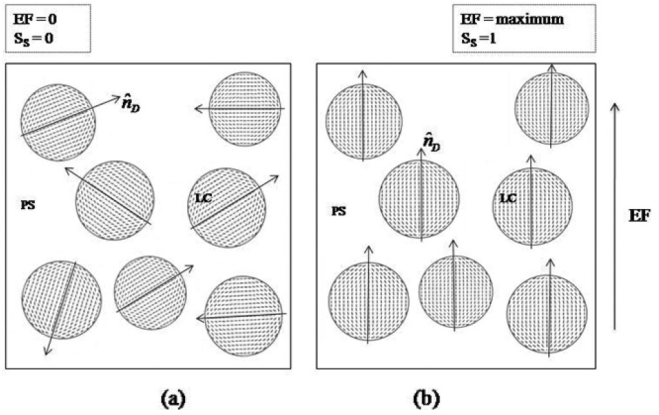

FIG. 7. Orientation of LC droplets inside a PS matrix. (a) Droplet directors are randomly oriented in the absence of an external EF; (b) droplet directors are aligned in the direction of an applied EF.

conductivities when the LC molecules aligned in the direction parallel to the EF, at which $\kappa_{PDLC} = \kappa_{PDLC\parallel}$ and $\kappa_{LC} = \kappa_\perp + \frac{1}{3}\Delta\kappa(1 + 2\,S_D)$ with $S_D = 0.7$ (Fig. 7).

Table I contains the thermal conductivity values used for calculations and the results obtained for γ values. These values indicate that the apparent thermal resistances due to the Kapitza resistance are lower for both of the samples, but not negligible. Moreover it is less prominent in the 85% LC sample than the 73% LC sample. The latter could be due to the reduction in droplet size at low LC concentrations, which in principle increases the ratio, γ, for a same Kapitza radius. Interestingly, these values are comparable to the one found previously for PS/5CB composites [7].

B. PDLC under a frequency-varying electric field

Subsequently we have investigated the depolarization field effects in PDLC samples by varying the frequency of the applied EF, f_e, while fixing the amplitude at a minimum value in order to attain a maximum κ_{PDLC} at $f_e = 1$ kHz. Figures 8(a) and 8(b), respectively, show the thermal diffusivity and thermal conductivity of the PDLC sample with 85% LC as a function of f_e at constant EF of 0.127 V/μm (determined from the EF-varying experiments). The experiments (as a function of f_e) were conducted successively at 18, 20, 22, and 30 Hz of laser modulation frequencies (f) and filtered the data by plotting ρC (Fig. 9) while taking the points lying within $\pm 0.65\%$ from the mean value.

Results on thermal diffusivity and conductivity as a function of f_e for PDLC with 73% LC are also displayed in Figs. 8(c) and 8(d), respectively. The results are obtained by taking the mean of three f_e scans, at the same $f = 18$ Hz. Here also the data were filtered by plotting ρC (Fig. 9) and taking the points

TABLE I. Parameters of PDLC samples.

LC vol. % (x)	$\kappa_{PDLC\parallel}$	$\kappa_{LC\parallel}$	ϕ_{LC}	γ	r_d (μm)
85%	0.179	0.24[a]	0.78	0.03	0.5–2.5
73%	0.138	0.24[a]	0.55	0.1	0.25–1

[a]Reference [27].

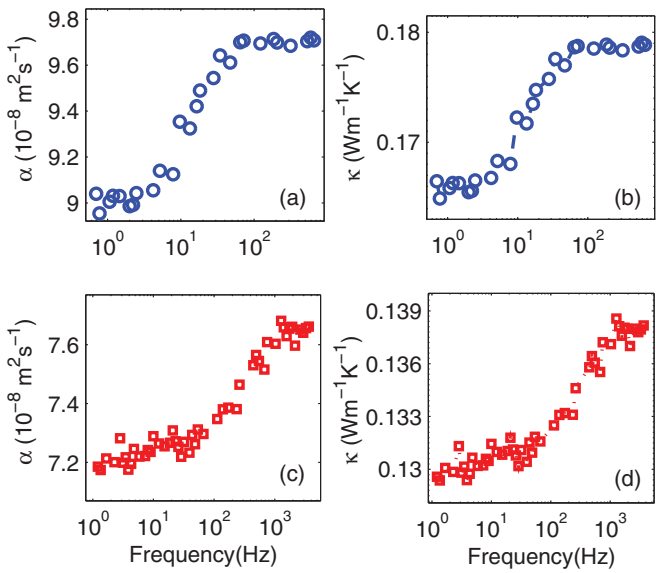

FIG. 8. (Color online) Experimentally observed thermal diffusivities (a and c) and conductivities (b and d) for PDLC 85% (a and b) and for PDLC 73% (c and d) as a function of f_e. Applied EF for PDLC 85% and for PDLC 73% were 0.127 and 0.18 V/μm, respectively.

lying within $\pm 0.9\%$ (the filtering range was chosen in a way which gives enough data points) of the ρC mean value.

Plotted ρC data, for both PDLC samples, are unaffected by the frequency of applied EF as expected. These results clearly show the frequency dependence of the dynamic thermal properties of PDLC samples. At relatively high frequencies, depending on the LC concentration, the charge accumulation at the LC-polymer interfaces is interrupted, and the effects of the depolarization field vanish. This makes the molecules better aligned in the direction of the EF, and hence the heat transport also increases and reaches its maximum. On the other hand, the dominant depolarization field distorts the heat flow at low frequencies.

1. *Effective thermal conductivity of LC droplets*

Originally the change in thermal conductivity comes from the reorientation of the LC droplet directors in the direction

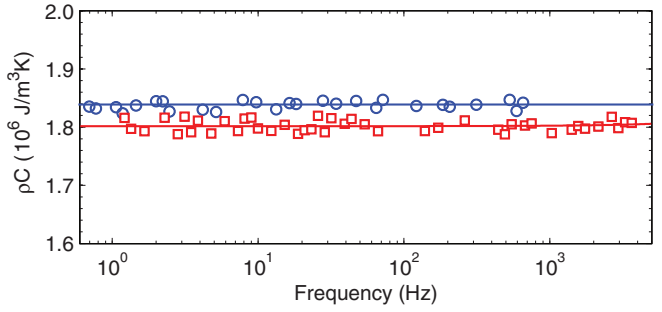

FIG. 9. (Color online) Volumetric heat capacity of PDLC samples with 85% LC (blue circles) and 73% LC (red squares) as a function of f_e. The solid lines represent the mean values of ρC for each sample.

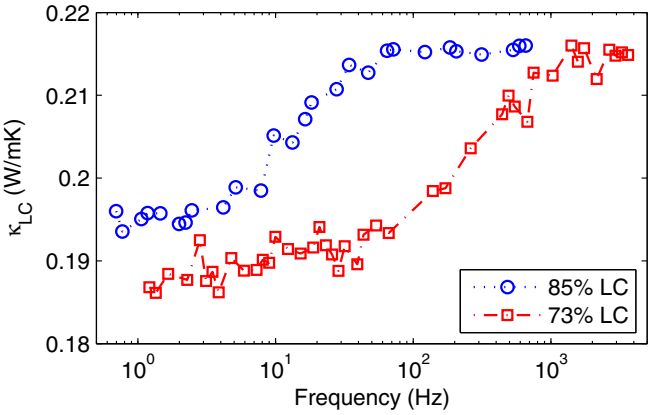

FIG. 10. (Color online) Average thermal conductivity of liquid crystal droplets as a function of f_e. Blue circles show the result for the 85% LC and red squares for the 73% LC sample.

of the heat flow, inside the polymer matrix. Therefore, using Eq. (7), one can estimate the mean thermal conductivity of LC droplets, given by

$$\kappa_{\mathrm{LC}} = \frac{1}{\kappa_{\mathrm{PDLC}}} \times \frac{\kappa_m[2\kappa_m(1-\phi) - \kappa_{\mathrm{PDLC}}(2+\phi)]}{[(1+2\gamma) - \phi(1-\gamma)] - \kappa_m[1+2\gamma+2\phi(1-\gamma)]}. \tag{10}$$

Evolution of the mean thermal conductivity of LC droplets, κ_{LC}, for PDLC samples of 73% LC and 85% LC is shown in Fig. 10. Calculations are done using the values of γ and ϕ_{LC} in Table I.

2. *Frequency-dependent thermal conductivity and MWS effect*

The relation between droplet electric field, E_{drop}, and the sample order parameter, S_S, is given by [32]

$$S_S = \frac{1}{4} + \frac{3(e^2+1)}{16\,e^2} + \frac{3(3\,e^2+1)(e^2-1)}{32\,e^3} \ln\left|\frac{e+1}{e-1}\right| \tag{11}$$

with e being the reduced field parameter which can be expressed as $e = E_{\mathrm{drop}}/E_0$. E_0 is the threshold EF (the field necessary to reorient LC molecules in the preferred direction), and its value depends on parameters such as the LC droplet's radius (r_d), shape, elastic free energy, surface anchoring and dielectric properties of the LC material, and polymer matrix. For nematic LC droplets, confined to a small spherical volume, the surface-to-volume ratio is relatively high. Thus, the droplet director configuration strongly depends on the interplay between bulk elastic forces and surface interactions. Considering constant and strong anchoring conditions, an approximated relation for E_0 is given by [17]

$$E_0 \approx \frac{1}{r_d}\sqrt{\frac{K}{\epsilon_0 \Delta\epsilon}}, \tag{12}$$

where ϵ_0 is the permittivity of free space (8.85×10^{-12} F/m), $\Delta\epsilon$ is the dielectric anisotropy, and K is the effective elastic constant of LC droplets.

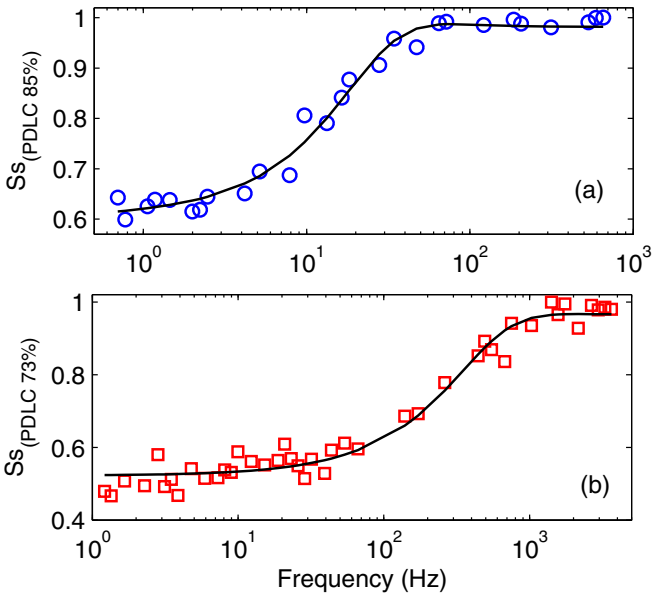

FIG. 11. (Color online) PDLC order parameter vs f_e. (a) PDLC 85%; EF $= 1.27 \times 10^5$ V/m; circles (blue) show the experimentally found S_S, and the solid line is the best fit. (b) PDLC 73%; EF $= 1.8 \times 10^5$ V/m; squares (red) show the experimentally found S_S, and the solid line represents the best fit.

In order to establish the relation for the effective thermal conductivity variations of PDLCs as a function of frequency of the applied electric field, one can insert the equation for E_{drop} (f_e) [Eq. (1)] into the equation for the sample order parameter [S_S, Eq. (11)], and the resultant then put into the expression for LC droplet thermal conductivity [κ_{LC}, Eq. (9)] and finally to the expression for κ_{PDLC} (f_e) [Eq. (7)], as shown by

$$E_{\text{drop}}(f_e) \overset{\text{Eq. (1)}}{\rightarrow} S_S \overset{\text{Eq. (11)}}{\rightarrow} \kappa_{\text{LC}} \overset{\text{Eq. (9)}}{\rightarrow} \kappa_{\text{PDLC}}(f_e).$$

The outcome of the above relation for $\kappa_{\text{PDLC}}(f_e)$ can be used to model the frequency-dependent effective thermal conductivity results of PDLC samples (Fig. 4) to find electrical LC parameters and polymer matrix as well as the threshold electric field E_0.

Figure 11 shows the experimentally found order parameter, S_S (circles), along with the numerical fit (full line) for PDLC 85% LC and 73% LC samples as a function of frequency of the applied EF. The order parameter is calculated from the experimental thermal conductivity of PDLC, κ_{PDLC}, by rearranging Eq. (9) for S_S and using Eq. (10). During the fitting procedure, E_0 as well as the electrical conductivities of both the polymer matrix and LC are kept as free fitting parameters. Values of the materials' dielectric properties were taken from literatures. The results obtained from the fitting are shown in Table II.

TABLE III. Elastic constants for the PDLC samples.

x	$\Delta\epsilon$	$r_d(\mu\text{m})$	E_0 (V/m)	$K \times 10^{-12}$ (N)
85%	10	0.5–2.5	$(5.59 \pm 0.01) \times 10^4$	0.07–1.7
73%	10	0.25–1	$(7.93 \pm 0.02) \times 10^4$	0.03–0.5

The threshold fields (E_0) or the threshold frequencies (f_0) found from the experiments show decreasing behavior with respect to the increase in LC concentration. This is expected, and it can be explained in relation to the increase in droplet size [see Eq. (12)] due to the increase in LC concentration. Knowing E_0 and the average droplet size, we can deduce the elastic constant, K, using Eq. (12). The range of values found for K, depending on their droplet radius, for both of the PDLC samples is shown in Table III. These values are lower than the reported values for bulk nematic 5CB (4.1×10^{-12}) [28], even though the K values are much closer to the bulk values for the biggest droplets. The electrical conductivity values for PS and LC found from the 85% LC experimental data are in good agreement with the values found in the literature (see Sec. III), while for the 73% LC sample, the results show relatively higher electrical conductivity values than reported. The differences in electrical conductivity values between the two samples can be mainly due to the change in LC solubility in PS, which can significantly affect the ionic concentration inside the material. For an increased ionic concentration in LCs, the conductive shielding also increases. This will reduce the effective EF acting on LC droplets. The variations in the elastic and electric parameters can also be due to a number of other factors that are not taken into account in our studies due to the complexity. Among these, anchoring forces and droplet shape anisotropy have a significant role in defining the threshold EF.

VI. CONCLUSION

The Maxwell-Wagner-Sillars polarization effects on thermal transport through PDLCs have been investigated with two samples (5CB/PS) containing 73% and 85% volume fractions of LCs in PS using an improved PTR technique. Experiments are done by (i) varying the amplitude of the electric field at fixed frequency as well as (ii) varying the frequency of the electric field at constant amplitude. The results on effective PDLC thermal conductivities versus amplitude of the applied EF are used to calculate γ, a parameter which describes the contribution of LC droplet volume in heat transport through it. The determined γ values show that the volume of the LC droplet is involved in the thermal transport.

Results on the thermal conductivity of PDLCs as a function of a frequency-dependent electric field (at constant amplitude) clearly show the thermal transport through PDLC materials is

TABLE II. Electrical parameters of PDLC samples from MWS fit.

x	σ_M (S/m)	σ_{LC} (S/m)	E_0 (V/m)	f_0 (Hz)	E_a (V/m)
85%	$(6.45 \pm 0.03) \times 10^{-9}$	$(1.217 \pm 0.005) \times 10^{-7}$	$(5.59 \pm 0.01) \times 10^4$	7.0 ± 0.9	1.27×10^5
73%	$(1.195 \pm 0.006) \times 10^{-7}$	$(1.203 \pm 0.006) \times 10^{-6}$	$(7.93 \pm 0.02) \times 10^4$	377 ± 12	1.80×10^5

affected by interfacial polarization field effects. The thermal conductivity data is used to plot PDLC order parameter, S_S. Existing theories are used to model the frequency-dependent PDLC order parameter and extracted the threshold electric field, E_0, as well as the electrical conductivities of both the LC and polymer matrix. The results for the electrical conductivities from 85% LC sample are closer to the already reported values, while for the 73% LC sample they show an order of magnitude higher values. We concluded that the difference in values are mainly coming from the increase in ionic concentrations as well as due to the variations in anchoring forces and droplet shape. Recent work has investigated the effect of anchoring forces on the electro-optical behavior of PDLC with bipolar and radial droplet configurations [34]. It shows that these configurations influence the MWS effect in PDLCs. In the future, we will focus on thermal properties of PDLCs with a radial droplet configuration.

ACKNOWLEDGMENTS

The authors thank Prof. A. Daoudi and Prof. F. Roussel for fruitful discussions. This work was financially supported by the M.E.S.R.

[1] J. L. Fergason, SID Int. Symp. Dig. Tech. Pap. **16**, 68 (1985).
[2] J. W. Doane, N. A. Vaz, B.-G. Wu, and S. Zumer, Appl. Phys. Lett. **48**, 269 (1986).
[3] F. Basile, F. Bloisi, L. Vicari, and F. Simoni, Phys. Rev. E **48**, 432 (1993).
[4] Y.-H. Lin, H. Ren, and S.-T. Wu, Appl. Phys. Lett. **84**, 4083 (2004).
[5] V. K. S. Hsiao and W.-T. Chang, Appl. Phys. B **100**, 539 (2010).
[6] V. A. Loiko and A. V. Konkolovich, J. Exp. Theor. Phys. **103**, 935 (2006).
[7] A. Hadj Sahraoui, S. Delenclos, S. Longuemart, and D. Dadarlat, J. Appl. Phys. **110**, 033510 (2011).
[8] M. Kuriakose, M. Depriester, D. Dadarlat, and A. H. Sahraoui, Meas. Sci. Technol. **24**, 025603 (2013).
[9] R. W. Sillars, J. Inst. Elec. Eng. **80**, 378 (1937).
[10] K. W. Wagner, Arch. Elektrotech. **2**, 371 (1914).
[11] R. M. Soliman, Ph.D. thesis, Universität Rostock, 2005.
[12] M. Boussoualem, R. C. Y. King, J.-F. Brun, B. Duponchel, M. Ismaili, and F. Roussel, J. Appl. Phys. **108**, 113526 (2010).
[13] J. Han, J. Korean Phys. Soc. **43**, 45 (2003).
[14] M. Boussoualem, F. Roussel, and M. Ismaili, Phys. Rev. E **69**, 031702 (2004).
[15] M. Boussoualem, M. Ismaili, J.-F. Lamonier, J.-M. Buisine, and F. Roussel, Phys. Rev. E **73**, 041702 (2006).
[16] J. R. Kelly and D. L. Seekola Proc. SPIE **1257**, 17 (1990).
[17] P. S. Drzaic, *Liquid Crystal Dispersion* (World Scientific, Singapore, 1995).
[18] F. Roussel, J. Buisine, U. Maschke, X. Coqueret, and F. Benmouna, Phys. Rev. E **62**, 2310 (2000).
[19] F. Benmouna, A. Daoudi, F. Roussel, J.-M. Buisine, X. Coqueret, and U. Maschke, J. Polymer Sci. B **37**, 1841 (1999).
[20] G. W. Smith, Mol. Cryst. Liq. Cryst. Incorp. Nonlin. Optics **180**, 201 (1990).
[21] G. Perrier and A. Bergeret, J. Appl. Phys. **77**, 2651 (1995).
[22] D. R. Lide, *CRC Handbook of Chemistry and Physics*, 78th ed. (CRC Press, Boca Raton, FL, 1997).
[23] B. Gestblom and S. Wrobel, Liq. Cryst. **18**, 31 (1995).
[24] V. Allouchery, Ph.D. thesis, Université du littoral côte d'Opale, Dunkerque, France, 2000.
[25] T. Bouchaour, F. Benmouna, F. Roussel, J.-M. Buisine, X. Coqueret, M. Benmouna, and U. Maschke, Polymer **42**, 1663 (2001).
[26] A. Boudenne and S. Khaldi, J. Appl. Polym. Sci. **89**, 481 (2003).
[27] M. Marinelli, F. Mercuri, U. Zammit, and F. Scudieri, Phys. Rev. E **58**, 5860 (1998).
[28] J. W. Doane, A. Golemme, J. L. West, J. B. W., Jr., and B. G. Wu, Mol. Cryst. Liq. Cryst. Incorp. Nonlin. Optics **165**, 511 (1988).
[29] M. Kuriakose, Ph.D. thesis, Université du Littoral Côte d'Opale, 2013.
[30] C.-W. Nan, R. Birringer, D. R. Clarke, and H. Gleiter, J. Appl. Phys. **81**, 6692 (1997).
[31] S. Zumer and J. W. Doane, Phys. Rev. A **34**, 3373 (1986).
[32] J. R. Kelly and P. Palffy-muhoray, Mol. Cryst. Liq. Cryst. Sci. Tech. A **243**, 11 (1994).
[33] F. Simoni, in *Nonlinear Optical Properties of Liquid Crystals and Polymer Dispersed Liquid Crystals*, edited by H. L. Ong, Series in Liquid Crystals, Vol. 2 (World Scientific, Singapore, 1997), Chap. 5, pp. 176–216.
[34] M. Boussoualem, M. Ismaili, and F. Roussel, Soft Matter **10**, 367 (2014).